Although we have shown that proline can induce a hyperplasia of the bile duct, we have not definitely established that this is the mechanism by which *Fasciola* establishes itself in its mammalian host. Studies with the proline analog, 1-azetidine-2-carboxylic acid (*12*), should answer this question. Should the proline inhibitor fail to interfere with establishment of *Fasciola* in the bile duct or with enlargement of the main bile duct when the flukes are implanted in the abdominal cavity, then some other mechanisms may be operating. However, an inhibitory effect by proline inhibitors would strongly support the hypothesis that proline is the mediator of the hyperplastic response in fascioliasis. In any event, investigations of the effects of 1-azetidine-2-carboxylic acid on *Fasciola* infections should be of interest in determining a possible therapeutic role for this compound. Indeed, Senft (*13*) suggested that proline analogs be tested for their activity against the human blood fluke *Schistosoma* which is also rich in free proline.

If proline is the agent which induces hyperplasia of the bile duct in fascioliasis, it is likely that this mechanism of bile duct enlargement occurs in other liver fluke diseases since high levels of free proline have been found in all trematodes examined thus far.

HADAR ISSEROFF
JOSEPH T. SAWMA
DAVID REINO

Department of Biology,
State University College at Buffalo,
Buffalo, New York 14222

References and Notes

1. K. B. Sinclair, *Helminth Abstr.* **36**, 115 (1967).
2. H. F. Hsü, *Chin. Med. J.* **55**, 542 (1939); *ibid.* **56**, 122 (1939); B. Dawes, *Nature (London)* **198**, 1011 (1963).
3. B. Dawes, *Parasitology* **53**, 123 (1963).
4. H. Isseroff, P. R. Girard, M. D. Leve, *Exp. Parasitol.* **41**, 405 (1977).
5. H. Isseroff, M. Tunis, C. P. Read, *Comp. Biochem. Physiol.* **41B**, 157 (1972).
6. B. Kurelec and M. Rijavec, *ibid.* **19**, 525 (1966).
7. J. Ertel and H. Isseroff, *J. Parasitol.* **60**, 574 (1974); *Rice Univ. Stud.* **62**, 97 (1976).
8. A. Huberman, A. Recio, M. Rojkind, *Proc. Soc. Exp. Biol. Med.* **131**, 200 (1969); M. Rojkind and L. Diaz de Leon, *Biochim. Biophys. Acta* **217**, 512 (1970); M. Chvapil and J. N. Ryan, *Agents Actions* **3**, 38 (1973).
9. H. Popper, F. Paronetto, F. Schaffner, V. Perez, *Lab. Invest.* **10**, 265 (1961).
10. J. T. Sawma, H. Isseroff, D. Reino, in preparation.
11. R. R. Sokal and F. J. Rohlf, *Biometry* (Freeman, San Francisco, 1969).
12. L. Fowden and M. H. Richmond, *Biochim. Biophys. Acta* **71**, 459 (1963).
13. A. W. Senft, *Ann. Trop. Med.* **59**, 164 (1965).
14. This research was supported in part by grant AI-09911 from the NIAID. We thank W. Schefler for advice on statistics.

2 September 1977

Measurement of the Human Magnetic Heart Vector

Abstract. *A unipositional lead system has been developed to record the human magnetic heart vector and to permit comparison with the electric heart vector recorded with a conventional Frank lead system. Recordings made in five normal subjects showed a remarkably consistent relation between the electric and magnetic heart vectors. However, the angle between electric heart vector* R *and* T *waves was markedly different from the magnetic heart vector* R-T *angle. In addition, recordings made in two patients with bundle branch block showed a different relation between the electric and magnetic heart vectors compared to normal subjects. These data support the hypothesis that magnetic measurements have a different sensitivity to some components of cardiac activation compared with body surface potential measurements.*

Since the first recording of the magnetocardiogram (MCG) by Baule and McFee (*1*), considerable effort has been devoted to theoretical analysis of the magnetic field produced by cardiac electrical activity (*2*). While such analysis is complicated by the inhomogeneous nature of the human body, some investigators have concluded that the MCG contains information about intracardiac current sources that is unattainable from surface potential measurements alone (*3*, *4*). For instance, mathematical analysis shows that the electrocardiogram (ECG) is more sensitive than the MCG to cardiac current sources that are radial with respect to the cardiac center (*5*), whereas the MCG is primarily sensitive to tangential sources (*6*, *7*). This finding is applicable to a model of cardiac excitation that is based on a moving depolarization wave front which could be pictured as a double layer of charge, or on a model using distributed current dipoles (*4*).

Several studies have been made to determine whether such sensitivity differences might provide clinically useful MCG data. A-C coupled magnetometers with a typical bandwidth of 0.1 to 40 hertz have been used to record the magnetic field perpendicular to the chest wall (B_n) at multiple precordial locations (*8*, *9*). Such "maps" may aid in the analysis of local cardiac activation events, particularly in the free wall of the right ventricle and intraventricular septum (*9*). Mapping of B_n is analogous to detailed ECG mapping of body surface potentials (*10*) and reflects nondipolar as well as dipolar components of cardiac activation. A systematic analysis of the relation beteen maps of B_n and maps of ECG surface potentials does not appear to have been made.

A different approach to magnetocardiography suggested by Baule and McFee (*11*) is to measure the magnetic heart vector (MHV), which is related to the magnetic dipole moment of the heart. An ideal MHV lead system would detect the magnetic field from the tangential components of cardiac current in an element of myocardium with a sensitivity proportional to the distance of the active element from the cardiac center, and would be equally sensitive to cardiac events occurring in the anterior and posterior portions of the heart. The MHV obtained with such a lead system would have the advantage of being easily compared with the electric heart vector (EHV), such as commonly recorded with the Frank lead system for vector electrocardiography.

Baule and McFee measured the sagittal component of the MHV, but did not construct a lead system capable of measuring all three MHV components. Rosen and Inouye (*12*) recorded the vector magnetic field over the precordium and used the data at the instant of maximum signal to determine the components of a fixed magnetic dipole model. However, signal quality was not optimal, the distortions produced by the torso boundaries and inhomogeneities were not discussed, and apparently no attempt was made to compare these data with the vector electrocardiogram. Matelin (*13*) recorded two orthogonal MHV components. Wikswo (*14*) examined the temporal and spatial dependence of the vector magnetic field around the thorax and interpreted the data in terms of a moving magnetic dipole model.

To overcome the practical limitations of other MCG recording techniques, we have designed a "unipositional" lead system employing a SQUID (superconducting quantum interference device) differential magnetometer system located above the anterior chest wall of a supine subject, with the instrument axis through the estimated center of the ventricular chambers (*4*, *7*). Both pickup coils of the magnetometer are oriented at an angle of 54°44′ to the instrument axis so that three orthogonal components (B_A, B_B, and B_C) of the magnetic field can be recorded with successive 120° rotations of the magnetometer. A linear transformation converts these com-

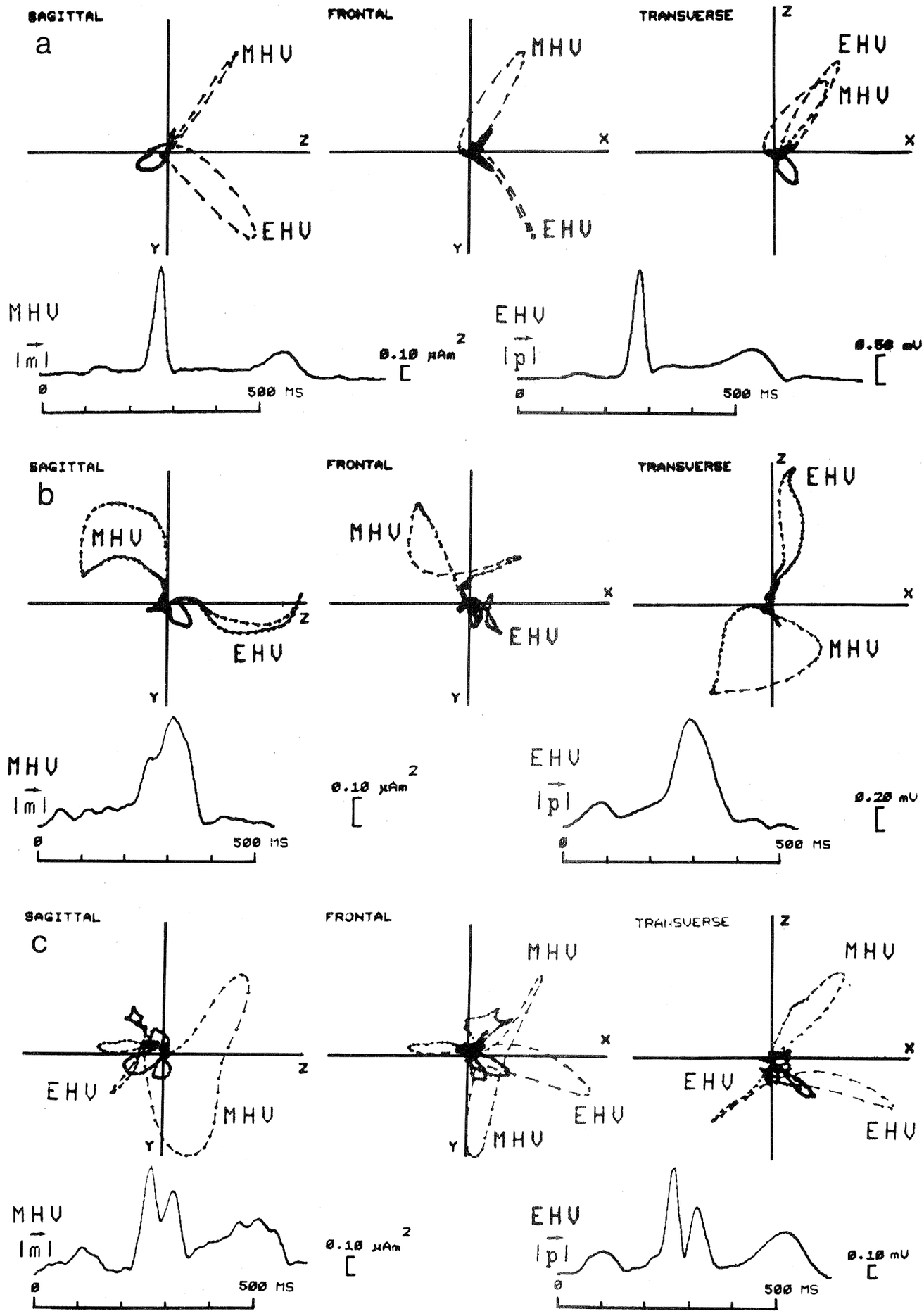
SAGITTAL
a
MHV
EHV
Z
Y
FRONTAL
MHV
EHV
X
Y
TRANSVERSE
Z
EHV
MHV
X
MHV
|m|
0.10 μAm²
0
500 MS
EHV
|p|
0.50 mV
0
500 MS
SAGITTAL
b
MHV
EHV
Z
Y
FRONTAL
MHV
EHV
X
Y
TRANSVERSE
Z
EHV
X
MHV
MHV
|m|
0
500 MS
0.10 μAm²
EHV
|p|
0.20 mV
0
500 MS
SAGITTAL
c
EHV
MHV
Z
Y
FRONTAL
MHV
X
EHV
Y
MHV
TRANSVERSE
Z
MHV
X
EHV
EHV
MHV
|m|
0
500 MS
0.10 μAm²
EHV
|p|
0.10 mV
0
500 MS

ponents to orthogonal components B_x, B_y, and B_z in an anatomically oriented coordinate system. Studies performed in an electrolytic tank model of an inhomogeneous torso indicate that, to a common scale factor, the true MHV (m_x, m_y, m_z) can be estimated from B_x, B_y, and B_z by correction factors of -2, -2, and $+1$, respectively (*7*). This system is not equally sensitive to anterior and posterior cardiac currents, however, and lead field studies show that the sensitivity of both m_x and m_y to the anterior right ventricular free wall are a factor of 2 greater than the sensitivity to the posterior left ventricular free wall (*7*).

Here we present data obtained with the unipositional lead system in five normal subjects and in two individuals with bundle branch block. The technical details of our magnetometer-signal processing system have been described (*14, 15*). Recordings were made with the subjects in a magnetic shield, and signal averaging of 15 to 20 beats further increased the signal-to-noise ratio. An EHV was recorded simultaneously with the Frank lead system. Figure 1a shows the EHV and MHV for a normal 31-year-old male, displayed in the standard EHV coordinate system where positive *X*, *Y*, and *Z* axes are left, inferior, and posterior, respectively. In the upper half of the figure the MHV and EHV vector loops in the left sagittal, frontal, and transverse planes are directed posteriorly and leftward, the MHV loop is directed superiorly, and the EHV loop is directed inferiorly. Each arrowhead represents a 4-msec real-time interval, with the arrowhead indicating the direction of change with time. The MHV calibration in microamperes-square meters and the EHV calibration in millivolts is also shown. In the lower half of Fig. 1a, the MHV magnitude $|\vec{m}|$ and the EHV magnitude $|\vec{p}|$, are plotted as functions of time, with P, QRS, and T wave detail clearly visible. Not shown, but also available, are the X, Y, and Z components of both signals. The plots of $|\vec{m}|$ and $|\vec{p}|$ are particularly valuable for identifying phases in the cardiac cycle when the MHV and EHV contain different information. For example, this subject shows more ST segment shift in the EHV than was seen in the MHV. The superimposed loop display in Fig. 1a clearly illustrates that, for this typical normal subject, the EHV and MHV loops in the sagittal and frontal planes are approximately perpendicular, while they are almost parallel in the transverse plane. The instantaneous angle between the EHV and MHV was 88° at the time of R wave peak and varied from 50° to 150° during QRS and T segments, with sudden changes at the S wave and at the end of the T wave. For comparison, the EHV and MHV of a point current dipole or a double-layer with a circular rim in a spherical conductor would be separated by a fixed angle of 90° (*4*).

On the basis of data from five normal subjects, the following comparisons between the MHV and EHV can be made: (i) In each individual the Y component of the EHV consistently resembled the Z component of the MHV. (ii) The vector loops in the left sagittal and frontal planes were approximately perpendicular, but in the transverse plane they were parallel to each other. For the five subjects, the average angle between the EHV and MHV at the *R*-wave peak was 94.5° ± 8.8° (standard error). [The perpendicularity of the EHV and MHV has been confirmed by Denis and Matelin (*16*).] (iii) The average angle between the MHV at the R-wave peak and the MHV at the T-wave peak (RT angle for the MHV) was 27.9° ± 6.4° and the RT angle for the EHV was 85.7° ± 10.3°. (iv) The average ratio of MHV magnitude at R wave to that at T wave (R/T ratio for the MHV) was 3.38 ± 0.48 and the average R/T ratio for the EHV was 3.26 ± 0.59.

Figure 1b shows an example of MHV and EHV recordings from a subject with left bundle branch block (LBBB), a left ventricular conduction defect. Figure 1c shows the corresponding data from a subject with right bundle branch block (RBBB). In LBBB, right ventricular activation proceeds in a relatively normal manner, but the left ventricle is activated later than normal and in an aberrant fashion. In RBBB, the opposite situation occurs. Thus, the initial portion of the QRS complex in classic RBBB reflects septal and relatively pure left ventricular activation, and the initial portion of the QRS in LBBB reflects septal and right ventricular activation. In both these patients, the ratio $|\vec{m}| / |\vec{p}|$ at 25 percent of QRS duration was less than that at 75 percent of QRS duration (LBBB: 0.28 versus 0.75 μa-m^2/mv; RBBB: 0.75 versus 1.21 μa-m^2/mv), suggesting that the MHV is more sensitive to cardiac currents during aberrant activation of either the left ventricle or right ventricle than is the EHV. The apparent increased magnitude of the MHV relative to the EHV during the later portion of the QRS may be due to a relative increase in the tangential components of current flow in the portion of the heart activated in an aberrant fashion. The data of Spach and Barr (*17*) on intramural potential distributions during ventricular activation in the dog during normal conduction and ectopic rhythms are consistent with this hypothesis.

These studies demonstrate the feasibility of clinical recording of the magnetic heart vector. Our data show that in normal subjects the RT angles for the MHV and EHV are markedly different, whereas the R/T ratios for the MHV and EHV are similar. This, and the finding of differences in the relations between the EHV and MHV in patients with aberrant ventricular activation, are consistent with theoretical predictions of an enhanced sensitivity of the MHV to certain cardiac electrical events, relative to the EHV. The observed differences between the electric and magnetic data lead us to conclude that the EHV-MHV relationship is not a simple one and may be influenced by cardiac abnormalities.

Fig. 1. (a) A computer-generated display of the magnetic heart vector (MHV) and electric heart vector (EHV) obtained from a representative normal subject. In the upper section, the vector loops in the left sagittal, frontal, and transverse planes are shown. In the lower section, the absolute magnitudes of the MHV, $|\vec{m}|$, and the EHV, $|\vec{p}|$, are plotted as functions of time. For the loops, each arrowhead indicates a 4-msec interval. See text for details. (b) MHV and EHV data obtained from a patient with left bundle branch block. Format as in (a), except QRS data only are presented. (c) MHV data from a subject with right bundle branch block. Format as in (a).

WILLIAM H. BARRY
WILLIAM M. FAIRBANK
DONALD C. HARRISON
KENNETH L. LEHRMAN
JAAKKO A. V. MALMIVUO
JOHN P. WIKSWO, JR.

Division of Cardiology, Stanford University School of Medicine, and Department of Physics, Stanford University, Stanford, California 94305

References and Notes

1. G. Baule and R. McFee, *Am. Heart J.* **55**, 95 (1963).
2. D. B Geselowitz, *Annu. Rev. Biophys. Bioeng.* **2**, 37 (1973); F. Grynzspan and D. B. Geselowitz, *Biophys. J.* **13**, 911 (1973); R. Plonsey, *IEEE Trans. Biomed. Eng.* **BME-19**, 239 (1972); H. Hosaka, D. Cohen, B. N. Cuffin, B. M. Horacek, *J. Electrocardiol. (San Diego)* **9**, 418 (1976).
3. D. B. Geselowitz, *J. Franklin Inst.* **296**, 379 (1973).
4. J. P. Wikswo, Jr., J. A. V. Malmivuo, W. H. Barry, M. C. Leifer, W. M. Fairbank, in *Cardiovascular Physics*, D. N. Ghista, E. Van Vollenhoven, W. Yang, Eds. (Karger, Basel, in press).
5. D. A. Brody, *Circ. Res.* **4**, 731 (1956).
6. R. McFee and G. Baule, *Proc. IEEE* **60**, 290 (1972).
7. J. A. V. Malmivuo, *Acta Polytech. Scand. Electr. Eng. Ser. No. 39* (1976); J. A. V. Malmivuo and J. P. Wikswo, Jr., *Proc. IEEE* **65**, 809 (1977).
8. D. Cohen and D. McCaughan, *Am. J. Cardiol.* **29**, 678 (1972); M. Saarinen, P. J. Karp, T. E.

Katila, P. Siltanen, *Cardiovasc. Res.* **8**, 820 (1974).
9. D. Cohen, E. Lepeshkin, H. Hosaka, B. F. Massell, G. Meyers, *J. Electrocardiol. (San Diego)* **9**, 398 (1976).
10. C. O. Eddelman, V. J. Ruesta, L. G. Horan, D. A. Brody, *Am. J. Cardiol.* **21**, 860 (1968).
11. G. Baule and R. McFee, *Am. Heart J.* **29**, 223 (1970).
12. A. Rosen and G. T. Inouye, *IEEE Trans. Biomed. Eng.* **BME-22**, 167 (1975).
13. D. Matelin, thesis, Université Scientifique et Médical de Grenoble (1974).
14. J. P. Wikswo, Jr., dissertation, Stanford University (1975); J. P. Wikswo, Jr., and W. M. Fairbank, *IEEE Trans. Magn.* **MAG-13**, 354 (1977).
15. J. P. Wikswo *et al.*, *Proc. San Diego Biomed. Symp.* **14**, 359 (1975); J. P. Wikswo, Jr., G. E. Crawford, W. H. Barry, W. M. Fairbank, D. C. Harrison, in *Computers in Cardiology*, H. G. Otrow and K. L. Ripley, Eds. (Institute of Electrical and Electronics Engineers Computer Society, Long Beach, Calif., 1976), pp. 317-321.
16. B. Denis and D. Matelin, personal communication.
17. M. S. Spach and R. C. Barr, *Circ. Res.* 37, 243 (1975); *ibid.*, p. 830.
18. We thank H. Burchell and M. Leifer for their comments. This work was supported in part by NSF/RANN grant APR72-03447-A04 and NIH grant HL-5866.

13 June 1977; revised 15 August 1977

Polymorphonuclear Leukocytes: Possible Mechanism of Accumulation in Psoriasis

Abstract. *Extracts of involved and uninvolved skin from nine patients with untreated psoriasis were studied for chemotactic activity. Psoriatic plaque contains increased amounts of a complement-dependent chemotactic factor that is inhibited by diisopropyl fluorophosphate. This factor may be human skin serine proteinase.*

Psoriasis is a common skin disease that is characterized clinically by sharply circumscribed, scaly red plaques. The epithelium of psoriatic lesions has an increased mitotic rate (*1*). One of the very early characteristic histological features is the presence of small microscopic foci of polymorphonuclear leukocytes (PMN's) in the stratum corneum (*2*). Tagami and Ofuji have shown that psoriatic scale contains leukotactic substances that may be products of complement activation (*3*). Proteinases extracted from tissue and cells are able to generate chemotactic peptides from complement (*4–6*). Several laboratories have demonstrated that psoriatic scale has an increased content of proteolytic enzymes (*7*). The experiments described here demonstrate that psoriatic plaque epidermis contains increased amounts of a serine proteinase which activates complement and induces PMN accumulation.

Elliptical biopsies (2.5 by 1 cm) of the rim of clinically active, nonpustular psoriatic plaques and normal appearing surrounding tissue were obtained under sterile conditions from the gluteal or thigh area of nine untreated psoriatic patients (*8*). Tissues were also obtained from five normal control subjects and one patient with pityriasis rubra pilaris. Sections of all specimens were removed for histological examination. The tissues were immediately trimmed of subcutaneous fat and placed in 2*M* KBr at 37°C for 30 minutes; the epidermis was easily removed from the underlying dermis by gentle traction (*9*). The epidermis preparations were washed five times in phosphate buffered saline (2 hours, 4°C) and then placed in 50 m*M* phosphate buffer, *p*H 7.5, containing 1*M* KCl and frozen and thawed five times. The tissue was extracted for 16 hours with gentle shaking at 4°C. The soluble extract was clarified by centrifugation (50,000*g*, 20 minutes, 4°C) and the extracted tissue pellet was frozen and assayed for DNA content (*10*). We have used the KBr epidermal preparation technique in previous work (*9*) and have documented that proteinase recovery is quantitative.

The clear supernatant solution was assayed for protein (*11*), the lysosomal proteinase cathepsin D (*9*), and neutral proteinase (*9*). The extract was then dialyzed against sterile saline and adjusted to a final protein concentration of 0.5 mg/ml. Chemotactic activity of the extracts was measured by assaying the accumulation of PMN's in the peritoneal cavity of mice according to the method of Snyderman *et al.* (*12*). Samples (2 ml) were injected into the peritoneal cavities of groups of normal and male mice deficient in the fifth component of complement, C5 (Jackson Laboratory). After 12 hours the animals were killed by inhalation of CO_2, and the peritoneal cavity was washed vigorously with 9 ml of Dulbecco's modified Eagle's medium with 10 percent fetal calf serum (Gibco) containing heparin (10 unit/ml). The peritoneal wash was counted for total number of white cells and for the percentage of PMN's by standard techniques. Results are expressed as absolute numbers of PMN's. At least two mice were injected with extracts of normal and psoriatic tissue from each of the nine patients. We had sufficient tissue in five patients to take portions of extract and incubate our preparations with 1 m*M* diisopropyl fluorophosphate (DFP) for 2 hours and then dialyzed them against three changes of physiological saline (12 hours, 4°C) before injection into the mice. Psoriatic extract was injected into three normal and three C5-deficient mice (*6*, *13*) from each of three patients. All chemotaxis experiments also included the injection of three mice with physiological saline, and the injection of three mice with proteose peptone (9 percent) (Difco), a complement-independent chemotactic agent. The chemotactic assay was demonstrated to be dose-dependent by injecting various dosages of purified proteinase into groups of three mice on three separate occasions (*14*).

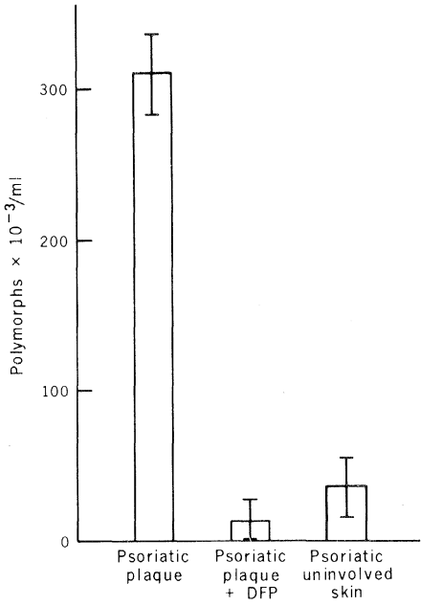

Fig. 1. Polymorph accumulation induced by injection of extracts of involved and uninvolved psoriatic skin (1 mg of protein per mouse) from nine patients. Results are expressed as the mean ± 1 standard error ($P < .01$); *DFP*, diisopropyl fluorophosphate.

Extracts of psoriatic plaque induced the accumulation of PMN's in the peritoneal cavity of normal mice (Fig. 1). This activity could be almost completely inhibited by prior incubation of the extracts with the serine proteinase inhibitor, DFP. Extracts of involved psoriatic skin induced significantly more accumulation of PMN's than extracts of uninvolved tissue ($P < .01$). Extracts of uninvolved psoriatic epidermis were slightly more effective in inducing PMN accumulation than extracts of control epidermis or epidermis from the patient with pityriasis rubra pilaris. Injection of equal amounts of psoriatic extract into normal and C5-deficient mice demonstrated that the enzyme evoked the ex-